Chapter 4

Carbon Quantum Dots: A Component of Efficient Visible Light Photocatalysts

Shan Cong and Zhigang Zhao

Additional information is available at the end of the chapter

http://dx.doi.org/10.5772/intechopen.70801

Abstract

Carbon quantum dots (CQDs) have been developed as a new member of nanocarbons, characterized by the relatively easy preparation from a wide spectrum of carbonaceous precursors through either bottom-up or top-down routes. Attractive optoelectronic properties have been observed with CQDs, including efficient light absorption, variable photoluminescence (PL), unique up-conversion PL and prominent electron transport ability, which make CQDs an important component with great potential in the design of efficient visible light-driven photocatalysts. In this chapter, detailed contribution of CQDs to the enhanced visible light-driven photocatalysis will be included, in the classification of the role as electron mediator, photosensitizer, spectral converter and sole photocatalyst.

Keywords: carbon quantum dots, photocatalysis, visible light, charge carrier, photoluminescence

1. Introduction

Carbon dots have emerged as a new class of quantum dot-like nanocarbons, which are typically constituted by discrete, quasi-spherical nanoparticles with sizes below 10 nm. The first discovery of quantum dot-like nanocarbons can be dated back to 2004, when carbon nanoparticles with sizes at about 1 nm were isolated by Xu et al. [1] as a byproduct of preparation of single-walled carbon nanotubes, separated from carbon soot produced by arc discharge. However, it was until 2 years later, these new kind of nanocarbons have been documented as "carbon quantum dots" (CQDs) and boosted widespread interests, since the synthesis of fluorescent carbon nanoparticles with diameter less than 10 nm from Sun's group [2].

Distinct from other well developed nanocarbons, such as fullerenes, carbon nanotubes and graphene, CQDs show their unique advantages, including isotropic shapes, ultrafine dimensions,

IntechOpen

© 2018 The Author(s). Licensee IntechOpen. This chapter is distributed under the terms of the Creative Commons Attribution License (http://creativecommons.org/licenses/by/3.0), which permits unrestricted use, distribution, and reproduction in any medium, provided the original work is properly cited. CC BY

tunable surface functionalities as well as the simple, fast and cheap preparations, which are attractive for a host of applications. Meanwhile, as a new member of quantum dot materials, CQDs also show potential as replacement for traditional toxic metal-based quantum dots currently in use, benefiting from their highly hydrophilic surface, high resistance to photobleaching, easy functionalization, chemical inertness, low toxicity and good biocompatibility. Until now, the applications of CQDs have been widely demonstrated in several fields, ranging from sensing, bioimaging to catalysis and energy conversion/storage.

This chapter will start with a brief overview about the preparation routes of CQDs, followed by a quick snapshot of their crystalline and electronic structure as well as the structure-induced optical properties. Then, the role of CQDs as an active component in modern visible light photocatalysis will be discussed in detail, based on a short review about works published in recent years.

2. Preparation methods

The preparation of CQDs can be generally classified into "top-down" and "bottom-up" routes (**Figure 1**). The former involves breaking down of carbonaceous materials via chemical, electrochemical or physical approaches. On the contrary, the latter is realized by carbonization of small organic molecules followed by chemical fusion. A detailed review about the preparation of CQDs can be found in several review articles [3–9], and only a brief overview of recent progresses about the CQDs preparation will be given here.

2.1. Top-down route

The first reported CQDs that isolated by chance from arc-discharged soot were produced by the top-down method, in which the carbonaceous soot was cleaved through nitric acid

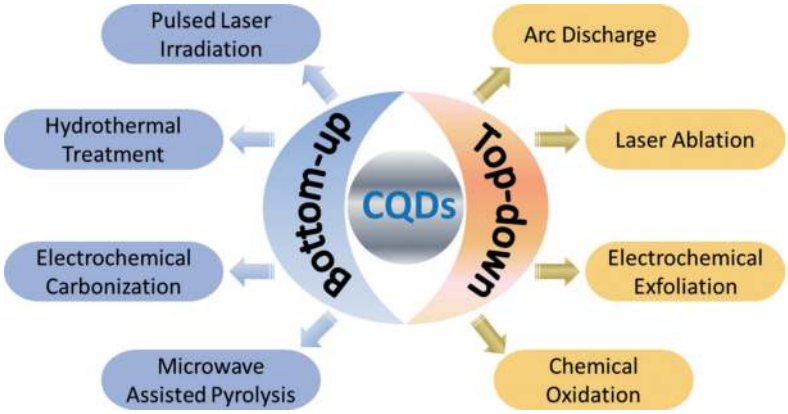

Figure 1. Schematic illustration of CQD preparation via "top-down" and"bottom-up" approaches.

oxidation, followed by gel electrophoresis separation to extract CQDs [1]. Subsequently, laser ablation of graphite using Ar as a carrier gas in the presence of water vapor was proved to be effective for the preparation of CQDs by means of the top-down route [2]. To date, CQDs have already been produced from graphite [10], graphene [11], carbon nanotubes (CNTs) [12] and other materials with sp2 carbon structure as a product of dimension reduction, meanwhile, through various physicochemical processes, including arc discharge [1], laser ablation [2], electrochemical exfoliation [13, 14] and chemical oxidation [15, 16]. However, to break down the chemical inert carbon structure of sp2 covalence bonds, the top-down process is invariably complicated with harsh conditions, some may be environmentally harmful, and thus not suitable for a large-scale production. In addition, effective control over the particle size of CQDs product is often difficult to realize in such top-down processes.

2.2. Bottom-up route

On the contrary, the bottom-up methods offer opportunities to control the growth of CQDs by using organic molecular as carbon precursors. Carbonization reaction can be applied to various kinds of molecules, followed by aggregation in solution to produce CQDs. Pulsed laser irradiation of toluene [17], hydrothermal treatment of citric acid [18], electrochemical carbonization of low-molecular-weight alcohols [19] and microwave-assisted pyrolysis of citric acid formamide solution [20] have already been utilized for the preparation of CQDs. Recently, biomass molecules, such as sucrose [21], glucose [22], cellulose [23] and amino acid [24], have attracted great attentions as suitable precursors for the preparation of CQDs via dehydrate and further carbonize. Moreover, raw biomass is also suitable precursor for the preparation of CQDs, as a strategy potential for large-scale production. For instance, Sahu et al. [25] prepared 0.4 g of CQDs from a mixture of orange juice with ethanol by hydrothermal treatment at 120°C for 2.5 h (**Figure 2A**). While using chicken eggs as raw material, Chen and coworkers [26] prepared CQDs via plasma-induced pyrolysis with a yield up to 10 g, suitable for applications as fluorescent inks (**Figure 2B**). In comparison with the liquid biomass as precursor, solid biomass may provide a more practical solution to scale up the synthesis of CQDs due to their much longer shelf life. For example, hair can be used as carbon source for the synthesis of CQDs, in utilization of its main component of keratin. A one-step thermal treatment of hair at 200°C for about 24 h was reported by Guo et al. to obtain CQDs, with the yield estimated to

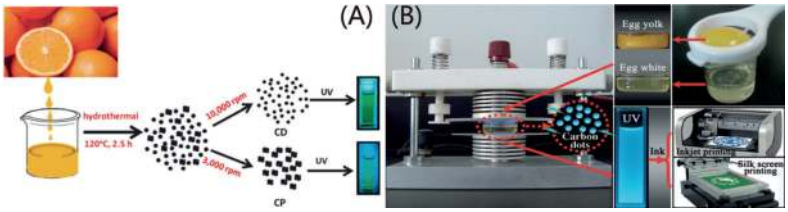

Figure 2. (A) Illustration of the formation of CQDs from orange juice by hydrothermal treatment. (B) Fabrication of CQDs from chicken egg and their application as fluorescent carbon inks. Reprinted with permission [25, 26]. Copyright 2012, Royal Society of Chemistry; Copyright 2012, Wiley-VCH.

be about 95% [27]. Thanks to the diversity and plenty of biomass, the large-scale synthesis of CQDs from biomass is of great potential especially in view of practical applications.

3. Structures and properties of CQDs

3.1. Structures

Generally, CQDs are quasi-spherical nanoparticles with diameter less than 10 nm, which can be amorphous or crystalline nanoparticles built up with sp2 carbon clusters. A typical fringe spacing of 0.34 nm can readily be distinguished from the high resolution transmission electron microscopy (HR-TEM) images of well crystalized CQDs, corresponding to the (002) interlayer spacing of graphite (**Figure 3A**) [28]. While as a special example of CQDs, graphene quantum dots (G-CQDs) usually possess a good crystallinity and layered structure (composed by less than 4, mostly a single graphene layer), with a crystal lattice spacing of 0.24 nm, corresponding to the (100) in-plane lattice parameter of graphene (**Figure 3B**) [29].

The modulated electronic structure of CQDs is unique among carbonaceous materials, which is dramatically size dependent. According to the quantum confinement effect (QCE), a reduced band gap of CQDs can be expected when the dot size increases. Li et al. [30] performed theoretical calculations to investigate the relationship between luminescence and cluster size of CQDs, who confirmed that the band gap reduced gradually as the size of CQDs increased (**Figure 3C**). Meanwhile, variable functional groups (such as hydroxyl and carboxyl) anchored on the surface of CQDs are indispensable for their excellent aqueous solubility, which can also greatly affect the electronic structure of CQDs. It has been demonstrated that different functional groups (either electron withdrawing or electron donating) simultaneously modulate the lowest unoccupied molecular orbital (LUMO) and highest occupied molecular orbital (HOMO) levels of CQDs, however, with relative small change in the band gap [31]. For instance, an electron donating group could raise both the HOMO and LUMO levels to higher energy, while an electron withdrawing group would cause a prominent down-shift of the total energy levels (**Figure 3D**). In addition, doping with heteroatoms such as nitrogen, sulfur were found to alter the electronic structures of CQDs significantly. The incorporation of ~1 at% of S into CQDs could effectively modify their electronic structure by introducing S-related energy levels between π and π^* orbitals of CQDs, which would diversify the electron transition pathways and facilitate inter band crossing of electrons (**Figure 3E**) [32].

Overall, the diversity of modulations for CQDs, from size control to surface functional groups exchange and heteroatom doping, makes it possible in the delicate control over their electronic structures and optical properties, showing potential as active components in light harvesting and utilizations.

3.2. Optical properties

Most notable, unique optical properties are discovered with CQDs, including wide-spectrum light harvesting from ultraviolet to near-infrared (NIR), tunable photoluminescence (PL) and

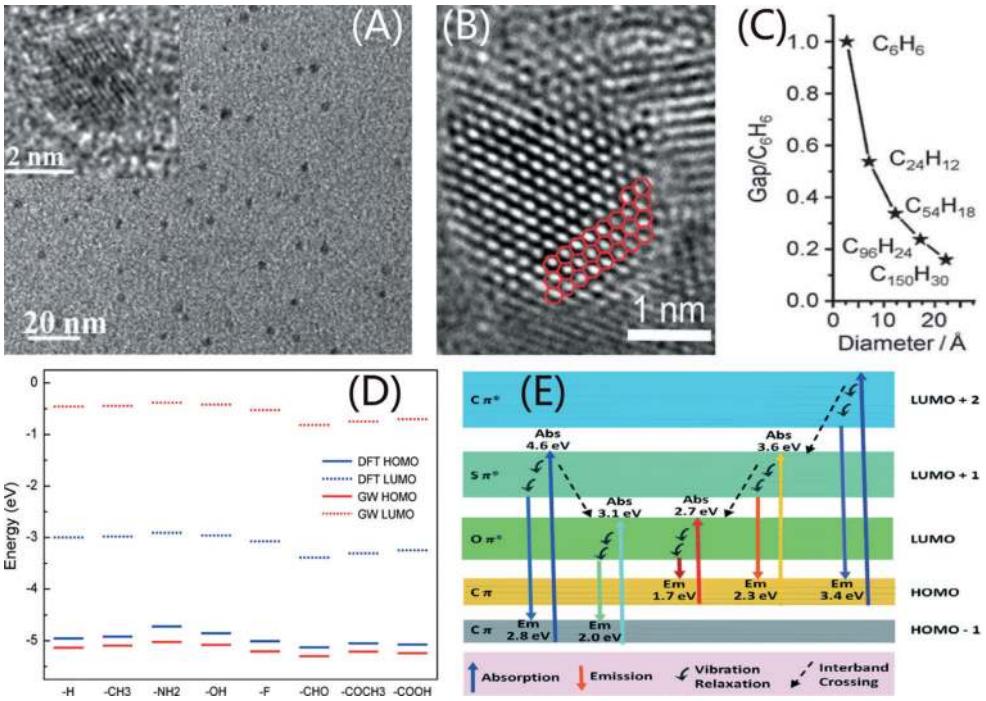

Figure 3. (A) TEM images of CQDs. (B) HR-TEM image of sp2 domains G-CQDs. (C) LUMO-HOMO gap dependence on the size of CQDs. (D) Energy diagrams of CQDs functionalized with different groups. (E) The proposed energy level diagram of S-doped CQDs. Reprinted with permission [28–32]. Copyright 2011, Wiley-VCH; copyright 2015, Royal Society of Chemistry; copyright 2010, Wiley-VCH; copyright 2015, American Chemical Society; copyright 2014, Royal Society of Chemistry.

efficient multiphoton up-conversion, all of which can be effectively tailored by the artificial control of the size, shape, surface and doping, based on the remarkable quantum confinement effect (QCE), surface effect and edge effect.

3.2.1. Absorbance

CQDs are effective photon-harvesting agents especially in short-wavelength region, due to the π-π* transition of C═C bonds. Typically, CQDs show strong optical absorption in the UV region (260–320 nm) with a tail extending into the visible range, in which a maximum peak around 230 nm is assigned to the π-π* transition of aromatic C═C bonds and a shoulder at 300 nm is assigned to the n-π* transition of C═O bonds or other surface groups [33]. In addition, the surface functional groups may also greatly contribute to the absorption at the UV-visible region, since a gradual red-shifted absorption can be observed after modification with some passivating agents. For instance, the absorbance of CQDs was found to increase to longer wavelength in the range of 350–550 nm after surface passivation with 4,7,10-trioxa-1,13-tridecanediamine (TTDDA) [34]. Moreover, doping with heteroatom is also effective to

tailor the absorption of CQDs. As reported by Qu et al. [35], the absorption band of S,N-co-doped CQDs moved into the visible region of 550–595 nm, showing potential as visible light-harvesting agent.

3.2.2. Photoluminescence (PL)

Tunable photoluminescence, with an emission peak ranging from deep ultraviolet to visible or even NIR region, is one of the most fascinating features of CQDs. Usually, these observed tunable PL properties are in close relationship with the QCE or surface effects of CQDs.

It is wildly accepted that the PL of CQDs originates from the emissive surface energy traps upon stabilization, since surface passivation is often indispensable for photoluminescent CQDs with high quantum yield (**Figure 4A**) [36]. Meanwhile, some researchers suggested that the PL in CQDs may be a result of radiative recombination of surface-confined electrons and holes, based on the observation that PL of CQDs can be effectively quenched by both electron donors and acceptors [37]. Significantly, this notion indicates that photo-excited CQDs are both good electron acceptors and electron donors. While in some cases, quantum size effect is the main reason for the observed size-dependent optical properties of CQDs. As reported by Li et al. [30], CQDs emitted blue, green, yellow, and orange, respectively, along with increased dot size under identical λ_{ex} (**Figure 4B**). Since no appreciable change in the PL spectra after further H_2 plasma treatment to remove surface oxygen species, the luminescence emissions of CQDs was attributed to the quantum-sized graphite structure rather than the carbon-oxygen surface. However, contradict results also existed, as Bao et al. [28] observed a red-shifted PL emission peak when the sizes of CQDs decreased at the same λ_{ex}. Based on the assumption that smaller CQDs were easily oxidized to take on more oxygen-related surface states, they suggested the red-shifted PL of CQDs was a result of variations in surface states rather than a size effect.

Therefore, the origin of the displayed optical properties of CQDs is still in debate, which may be probably in relationship with the competition between the emissive sites and non-radiative trap sites on the surface, as well as the quantum confinement effects determined by particle sizes.

3.2.3. Up-conversion photoluminescence (UCPL)

In contrary to the conventional down-conversion fluorescence emissions (Stokes PL), certain CQDs are also found to display up-conversion fluorescence emissions (anti-Stokes PL), with the emission wavelength shorter than the excitation wavelength, arising from the simultaneous absorption of two or multiple longer wavelength photons. UCPL is an attractive optical property of CQDs, which enables many promising applications, especially for photocatalysis in the visible to NIR spectrum.

The visible emission of ~5 nm CQDs under the excitation of 800 nm femtosecond pulsed laser was first recorded by Cao et al. [38], who proposed a two-photon mechanism for the up-conversion emission. Later, several other groups observed similar UCPL from CQDs prepared via different synthetic routes. For instance, Gan et al. [39] demonstrated that blue light centered

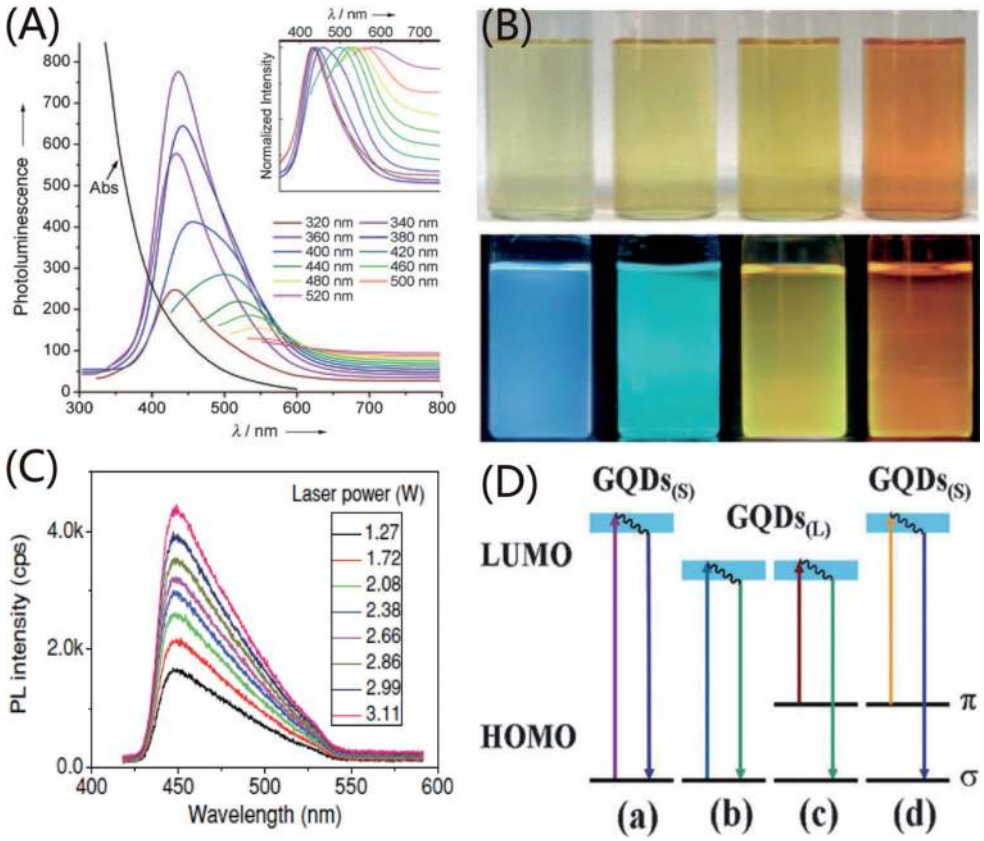

Figure 4. (A) UV/vis absorption (Abs) and PL emission spectra (recorded for progressively longer excitation wavelengths from 320 to 520 nm) of PEG_{1500N} passivated CQDs. (B) Optical images of CQDs illuminated under while (above, daylight lamp) and UV light (bottom, 365 nm). (C) UCPL spectra of CQDs under the excitation of a femtosecond pulsed laser at 800 nm. (D) Schematic illustration of various typical electronic transition processes of CQDs. Normal PL of small size (a) and large size (b); UCPL of large size (c) and large size (d). Reprinted with permission [30, 36, 39]. Copyright 2009, Wiley-VCH; copyright 2010, Wiley-VCH; copyright 2013, Wiley-VCH.

at 450 nm was emitted from CQDs under an excitation of 800 nm femtosecond pulsed laser, and the UCPL intensity was found to relate to the excitation power density (**Figure 4C**).

However, it was still under debate whether the multiphoton-active process was sufficient to explain the UCPL phenomenon of CQDs. In view of the practically constant energy difference of 1.1 eV between the excitation and emission, Shen et al. [40] proposed an anti-stokes transition mechanism using the energy level structural model, who postulated that low energy photons could excite π electrons (in intermediate levels) to LUMO followed by relaxation into σ orbital (HOMO) for the emission of a shorter wavelength photon (**Figure 4D**). Therefore, the constant energy difference here between excitation and emission light is ascribed to the energy gap between π and σ orbitals.

Moreover, Wen et al. [41] recently argued that the observed multiphoton excitation properties in some CQDs might be artificial and could originate from the normal fluorescence, which was excited by the second diffraction leaking in the monochromator of the fluorescence spectrophotometer. Therefore, great cautions should be paid to the observed UCPL of CQDs, and it was suggested that the exact up-conversion from CQDs would be excited under a high enough power density from a femtosecond pulsed laser.

4. Applications in photocatalysis

Based on the generation of charge carriers such as electrons and holes induced by photon absorption, photocatalysis has found great potentials in the application of both environmental remediation and energy conversion, ranging from pollutant degradation to H_2 generation and CO_2 reduction. To generate carriers with sufficient redox potentials, wide band gap semiconductors (such as TiO_2) are often used as photocatalysts, but at the cost of limited utilization of only high energy UV irradiation (~5% of sunlight). At the same time, recombination of charge carriers pervasively exists during their migration through the bulk to the surface in semiconductor particles, where to initiate photocatalytic reactions. Therefore, evolutions of photocatalytic system to overcome the low-usage of sunlight as well as high recombination rate of the photo-induced charge carriers is still an urgent need to improve the overall quantum efficiency for practical applications. Interestingly, all of the optical and structural properties of the CQDs mentioned above meet with the requirement of photocatalytic reactions (such as utilization toward solar spectrum, fast migration of charge carriers and efficient surface redox reactions), indicating the promising application of CQDs in photocatalysis. As a matter of fact, CQDs have shown their importance as a versatile component especially in visible light-driven photocatalysis since their discovery, ascribing to the tunable optical properties (such as absorbance, PL and UCPL) for excellent solar spectrum utilizations, also due to the electron accepting and transporting features of carbon nanomaterials that can direct the flow of photogenerated charge carriers. Therefore, CQDs can act not only as an efficient photocatalyst alone, but also as a multifunctional constituent in the design of photocatalyst for broadened light response and promoted electron-hole separation. In this section, we will summarize the fundamentally multifaceted roles of CQDs as an important component in visible light-driven photocatalysis.

4.1. Electron mediators

Photon-induced charge carriers with a sufficient amount that can migrate to the surface of semiconductors are at the core of photocatalytic reactions. Since charge carriers can easily be traps by various random defects, to collect or mediate the flow of charge carriers for efficient separation is necessary for an effective photocatalyst design. Noble metals with a large work function are commonly deposited onto the surface of semiconductors to act as an electron sink and help in an efficient separation of charge carriers. However, the use of noble metals shows a main drawback of poor economic viability due to their high expense. As a potential

electron mediator in placement of noble metals for new design of photocatalysts, CQDs show excellent electron conductivity as well as large electron-storage capacity, benefiting from the inherent sp2 graphitic carbon compositions.

On the one hand, CQDs can act as conductors for efficient charge carrier transport between adjacent semiconductors, due to the electron conductivity from the Ohmic contact at the semiconductor-CQDs interfaces. Miao et al. [42] fabricated a ternary visible light-driven photocatalyst with the construction of g-C_3N_4/CQDs/AgBr, by the in-situ growth of AgBr nanoparticles on CQDs modified g-C_3N_4 nanosheets. The nanocomposite exhibited improved photocatalytic efficiency for RhB degradation under visible irradiation (>420 nm), which was about 4.0, 5.3 and 2.3 times higher than that of AgBr, g-C_3N_4 and g-C_3N_4/AgBr, respectively. Due to the thermodynamically favorable electron transfer upon band alignment, CQDs was believed to act as mediators to promote the electron transfer from g-C_3N_4 to AgBr for an improved separation of electron-hole pairs, responsible for the improved photocatalysis (**Figure 5A**).

On the other hand, CQDs can act as electron sink to accept photogenerated electrons from adjacent semiconductors, and thus to suppress the electron-hole recombination, benefiting from the large electron-storage capacity of carbon nanostructures. Huang et al. [43] obtained CQDs/$ZnFe_2O_4$ photocatalysts via a simple hydrothermal route, which showed eight times larger transient photocurrent response in comparison with that of $ZnFe_2O_4$ alone under visible irradiation ($\lambda > 420$ nm). In a possible photocatalytic mechanism, the authors inferred that CQDs could function as an electron reservoir and transporter over CQDs/$ZnFe_2O_4$ hybrids, to improve both the separation and transfer efficiency of photogenerated charge carriers (**Figure 5B**). Wu et al. [44] demonstrated a case of a bi-quantum dot (QD) photocatalyst for overall water splitting, in which CQDs and $BiVO_4$ QDs were combined together. Without any co-catalysts or sacrificial reagents but under solar light irradiation, H_2 evolution of 0.92 μmol h^{-1} was achieved with such hybrids, about four times that of $BiVO_4$ QDs. In such a two-electron pathway reaction, CQDs and $BiVO_4$ QDs were believed to be reduction and oxidation reaction

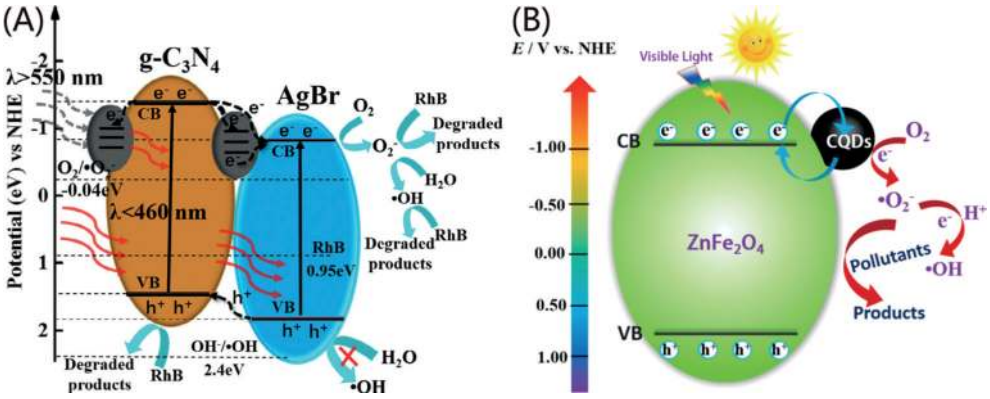

Figure 5. (A) CQDs as electron conductor at the interface of C_3N_4 and AgBr. (B) CQDs as electron sink at the surface of $ZnFe_2O_4$. Reprinted with permission [42, 43]. Copyright 2017, Elsevier; copyright 2017, American Chemical Society.

center, respectively. As an effective electron acceptor, CQDs received electrons from VB of $BiVO_4$ before transferring to surface-adsorbed water for hydrogen production.

Therefore, as electron mediators, CQDs show noble metal comparable ability as both conductor and sink for an efficient charge separation in association with semiconductor photocatalysts. At the same time, the relative low cost and easy preparation make CQDs an available alternative to the expensive noble metal as electron mediators in new design of photocatalysts.

4.2. Photosensitizers

Extending light harvesting, especially by increasing the absorbance of visible photons, has been a popular strategy to achieve improved efficiency for modern photocatalysis. While the extended absorption spectrum of semiconductors usually means narrowed bandgap and thus decreased redox ability, which often obstructs the design of visible light-driven photocatalysts. Using visible light photosensitizers that can transfer photogenerated electrons to the CB of semiconductor in contact has been widely employed to address this conflict. Quantum dots of CdS, CdSe, PbS, are well known photosensitizers with a relative narrow bandgap to achieve good light harvesting efficiency, however, still suffer from some inherent drawbacks, including high cost, instability against photocorrosion and dissolution of toxic heavy-metal ions. Recently discovered CQDs, as an intriguing member of the nanocarbon family, have shown great potentials as photosensitizers due to their broad absorption spectra and large absorption coefficients.

Zhang et al. [45] prepared CQDs with tunable size of 2–5 nm from graphitic polymeric micelles, which showed high water solubility due to the surface decorated carboxyl groups. The obtained CQDs were then loaded onto the surface of P25 TiO_2 through a facial dispersion-evaporation route, followed by thermal treatment at 300°C in air to remove organic passivation layer for a close contact at hetero interfaces. The cooperation of CQDs and TiO_2 was believed to be responsible for the visible light photocatalytic degradation of MB, since either CQDs or TiO_2 alone showed negligible activities. CQDs probably acted as a photosensitizer in the CQDs/TiO_2 hybrid, which injected visible light excited electrons into the CB of TiO_2, responsible for the remarkably enhanced visible light photocatalytic activity (**Figure 6A**). Wu et al. [46] suggested that the surface groups of CQDs were not necessarily removed before using as photosensitizers. CQDs with an average size of 30 nm were prepared through hydrothermal carbonization of pentosan, followed by the preparation of CQDs/TiO_2 composite through directly drying from the suspension of TiO_2 in a CQDs aqueous solution. The CQDs with abundant oxygen-containing groups could act as a photosensitizer to absorb visible light, with excited electrons transferred to the CB of TiO_2. These sensitized electrons then reacted with O_2 adsorbed on TiO_2 surface to produce active oxygen radicals (O_2^-), which were responsible for the observed MB degradation. In another case, Yu et al. [47] reported the efficient photocatalytic H_2 evolution activity of CQDs/P25 composite under both UV-vis and visible light ($\lambda > 450$ nm) irradiation without the aid of any noble metal cocatalyst. Different from pure P25, CQDs/P25 exhibited visible light-driven photocatalytic activity for H_2 production, ascribing to the photosensitizing ability of CQDs. Just like organic dyes, CQDs sensitized P25 into a visible light responsive "dyade" structure through the newly formed Ti—O—C bond, in

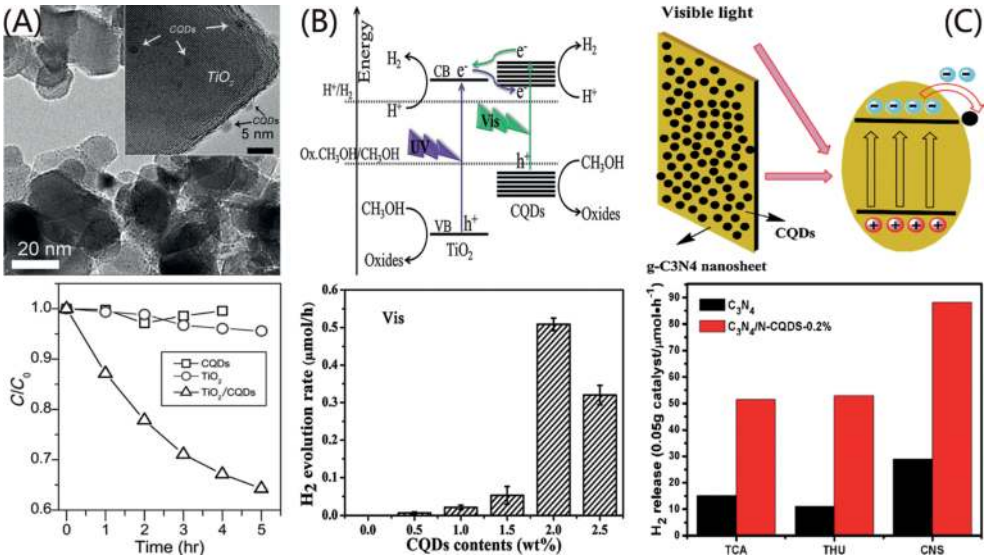

Figure 6. (A) TEM image of the TiO_2/CQDs hybrids and MB concentration (C/C_0) versus photocatalytic reaction time. (B) Schematic illustration for the H_2 production mechanism on the CQDs/TiO_2 under UV and visible light ($\lambda > 450$ nm), and photocatalytic H_2 evolution rates on CQDs/TiO_2 with varied CQDs contents under visible ($\lambda > 450$ nm) irradiation. (C) Schematic illustration of the C_3N_4/CQDs composites, and the phototcatalytic performance of C_3N_4 and 0.2 wt%-CQDs/C_3N_4 for the H_2 evolution rate under visible ($\lambda > 420$ nm) irradiation. Reprinted with permission [45, 47, 48]. Copyright 2015, Wiley-VCH; copyright 2014, Royal Society of Chemistry; copyright 2016, Elsevier.

which photo-induced electrons transferred from the excited CQDs to CB states of TiO_2, followed by reactions with protons for H_2 production (**Figure 6B**).

The characterized sp2 carbon composition of CQDs also contributes to the charge transfer ability as photosensitizers. In a recent report of Liu et al. [48], CQDs synthesized from bee pollens were used to couple with g-C_3N_4 nanosheets for a 2D/0D type photocatalysts via hydrothermal treatment. The composite has overcome the limited visible light absorption of C_3N_4, showing an optimal H_2 evolution of 88.1 μmol/h, 3.02 folds of pristine C_3N_4 nanosheets. Well dispersed CQDs uniformly anchored to the C_3N_4 nanosheets network via π-π stacking interactions were suggested to effectively expand the visible light absorption via photosensitization and hence suppress the recombination of photo-induced carriers (**Figure 6C**).

Overall, due to the excellent light harvesting ability over a broad spectrum, as well as the effective chemical binding toward semiconductor surface, carbon dots have shown their potential as alternatives to the scarce and toxic heavy-metal compounds that are currently used as photosensitizer for visible light harvesting.

4.3. Spectral converters

The UCPL of CQDs is of particular interests in this context, promising an emission of shorter wavelength photons upon the simultaneous absorption of two or multiple longer wavelength

photons. Such a spectral converting ability of CQDs provides an attractive strategy for the design of visible light- or even NIR-responsive photocatalysts. A large number of recent work concerning about the photocatalytic applications of CQDs have suggested the contribution of their UCPL properties. Ke et al. [49] used TiO_2 photocatalysts modified with CQDs to obtain a 3.6 times higher rate of MB degradation under visible light irradiation ($\lambda > 420$ nm) when compared with pure TiO_2, and the enhanced photocatalysis was mainly ascribed to the increased amount of oxidative radicals in hypothesis of the up-conversion process from CQDs (**Figure 7A**). Similar results have also been observed with CQDs/g-C_3N_4 hybrids, as shown by Zhang et al. [50]. After impregnation of CQDs into g-C_3N_4, a 3.7-fold enhancement in phenol degradation rate constant can be obtained compared with that of the pristine g-C_3N_4 under visible light irradiation ($\lambda > 400$ nm). As suggested by the authors, light of $\lambda > 550$ nm could be converted to $\lambda < 460$ nm photons by CQDs, and subsequently excited g-C_3N_4 to generate electron-hole pairs (**Figure 7B**). UCPL character of CQDs that enhanced the production of excitons by extending the visible light-absorption region was supposed to be one important contribution to the observed enhanced photocatalysis, along with the efficient charge separation arising from the band structure alignment.

However, some researchers clarified that UCPL of CQDs might not be the main reason for the improved photocatalytic activity after CQDs introduction. In a recent work of Di et al. [51], improved photocatalytic degradation of ciprofloxacin on N-CQDs/BiPO4 composite

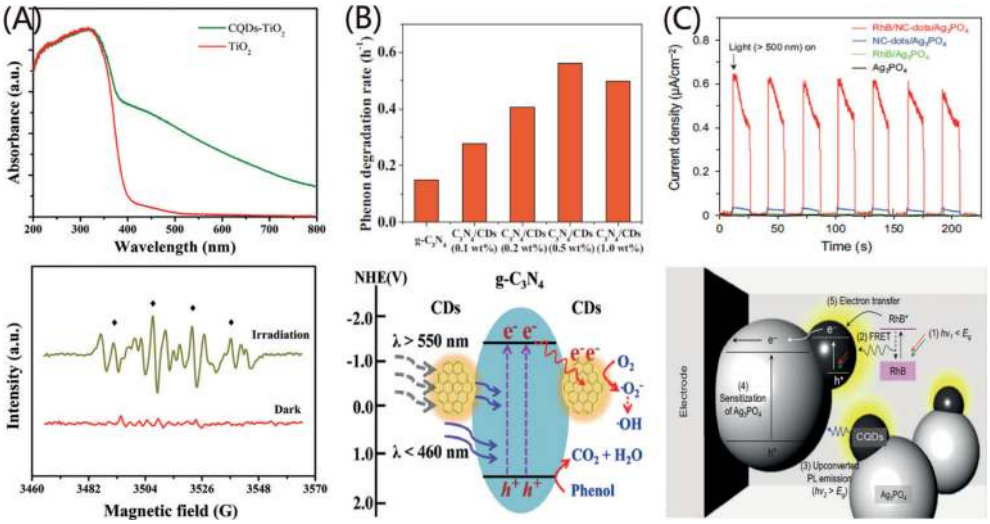

Figure 7. (A) UV-vis absorption spectra of TiO_2 and CQDs/TiO_2 hybrid, and the EPR spectra of hydroxyl radicals over the CQDs/TiO_2 hybrid under visible irradiation ($\lambda > 420$ nm). (B) Apparent rate constants of phenol degradation over CQDs modified C_3N_4 photocatalysts with varied loading amount, and the schematic illustration of the possible photocatalytic process on the C_3N_4/CQDs hybrid under visible light ($\lambda > 400$ nm). (C) Transient photocurrent responses at an applied potential of 0 V under visible irradiation ($\lambda > 500$ nm) for photocatalysts with different composition, and the schematic energy band diagram of the RhB/CQDs/Ag_3PO_4 nanocomposite. Reprinted with permission [49, 50, 52]. Copyright 2017, Elsevier; copyright 2016, Elsevier; copyright 2016, Elsevier.

was observed under UV irradiation, but only with negligible efficiency under visible light. Subsequently, the authors proposed that the up-converted PL may not play the crucial role for the improved activity in this system, instead, molecular oxygen activated by the oxygen defects on the surface of N-CQDs may be responsible for the organic removal under UV irradiation.

In fact, no direct evidence has been provided to confirm the contribution of UCPL to the improved photocatalytic activities postulated in many CQDs based photocatalytic systems. The generally poor efficiency of up-conversion process in most cases, if such an effect exists, may lead to its small influence compared to other optoelectronic contributions. Yu et al. [52] magnified the UCPL of CQDs by means of fluorescence resonance energy transfer (FRET)-assisted up-conversion process, in which rhodamine B (RhB) was combined with naked CQDs of 3.4 nm to make a FRET pair. The FRET effect was used to magnify the up-conversion of CQDs, with the up-converted photons subsequently sensitized Ag_3PO_4 particles and thus generating 18 times higher photocurrent at $\lambda > 500$ nm than those without RhB molecules (**Figure 7C**).

4.4. Sole photocatalyst

The origin of light absorption in CQDs stems from π-π^* (C═C) and n-π^* (C═O) transitions in the core and on the surface of the particles, respectively, which means that the optoelectronic properties of CQDs will be readily tuned by both size modulation and chemical modification. The size effect largely arises from the confinement, causing a separation of π and π^* orbitals prominently when the domain size is less than 10 nm. At the same time, CQDs rich in surface oxygen groups are usually p-doped due to the larger electronegativity of oxygen atoms relative to carbon atoms. Replacing oxygen functional groups on the CQDs surface with nitrogen-containing groups can readily transform CQDs into an n-type semiconductor. In addition to surface modification, direct substitution with heteroatoms in the graphene lattice also greatly affects the optical and electronic properties of CQDs. These excellent properties have gained CDs with an adjustable band structure together with broadband light-absorption ability, which inspire their applications as efficient photocatalyst.

Although CQDs alone as photocatalysts show great potential, relatively few examples of CQDs solely with satisfying photocatalytic activity have been recorded to date, partially due to the relative poor electron transfer inside the CQDs. Doping with heteroatoms has been proved to be an effective way to promote electron transfer and thus the performance of the CQDs as photocatalyst. Cu–N co-doping of CQDs was achieved by Wu et al. [53] through an one-step pyrolytic synthesis with Na_2[Cu(EDTA)] as precursor (**Figure 8A**). As a result of the Cu─N doping, the electron accepting and donating abilities of CQDs could be both enhanced, together with the increased electric conductivity. These merits ultimately facilitated the entire electron-transfer process in CQDs and further improved the photocatalytic oxidation of 1,4-dihydro-2,6-dimethylpyridine-3,5-dicarboxylate (1,4-DHP). In another case provided by Martindale et al. [54], N doped CQDs were synthesized by pyrolysis of aspartic acid (Asp) in air at 320°C. CQDs with N doping showed increased specific activity of 7950 μmol_{H2} $(g_{CD})^{-1}$ h^{-1} in the solar (AM1.5G) photocatalytic H_2 evolution system, with an

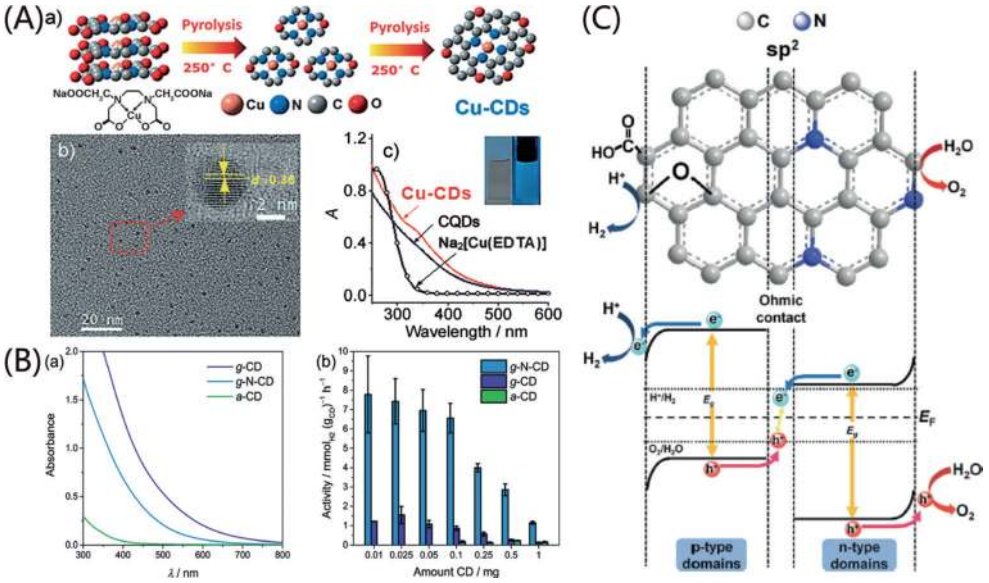

Figure 8. (A) (a) The synthetic procedure, (b) TEM images and (c) UV/vis absorption spectra of doped CQDs. (B) (a) UV/vis absorption spectra of N doped CQDs (g-N-CD), graphite CQDs (g-CD) and amorphous CQDs (a-CD), (b) photocatalytic H_2 generation with various amounts of CQDs (0.1–1 mg) under simulated solar irradiation (AM 1.5G, 100 mW cm^{-2}). Reprinted with permission [53–55]. Copyright 2015, Wiley-VCH; copyright 2017, Wiley-VCH; copyright 2014, Wiley-VCH.

order of magnitude improvement realized compared to undoped CQDs (**Figure 8B**). The authors suggested that nitrogen doping in CQDs increased the efficiency of hole-scavenging through electron donor effect and thereby significantly extended the lifetime of the photogenerated electrons.

Moreover, the electronic structure of CQDs can also be dramatically changed after heteroatomic doping. By treating GO in NH_3 at 500°C followed by oxidation with a modified Hummers' method, Yeh et al. [55] obtained N doped CQDs and applied as visible light ($\lambda > 420$ nm) driven photocatalyst for the overall water-splitting. Based on the electrochemical Mott-Schottky analysis, N doped CDs showed both p- and n-type conductivities, with the n-conductivity caused by embedding nitrogen atoms in the graphene frame and the p-conductivity by grafting oxygen functionalities on the graphene surface. The inherent sp2 clusters of CQDs served as the junction between the p- and n-domains to form buitin p-n diodes, which were responsible for an internal Z-scheme charge transfer at the QD interface, similar to that of biological photosynthesis (**Figure 8C**).

Therefore, by suitably adjusting the size, defect densities, atom doping and surface functional groups, it is possible to tune the electronic structure of CQDs and thus the optical response over a wide spectrum, allowing the potential application as effective photocatalysts with full utilization of the solar light.

5. Summary and outlook

After a decade of extensive investigation, CQDs have already been developed to be one of the most important members of modern nanocarbon family. Unexpected optoelectronic properties have been observed with this initially emergent nanocarbon material, including UV-visible absorbance, tunable PL and unique UCPL, together with electronic conductivity, showing the opportunity of further adjustment through surface functionalization and heteroatom doping. Specially, the excellent light harvesting capability and efficient photo-induced electron transfer ability make CQDs an exceptional candidate in visible light-driven photocatalytic applications, which play multifaceted roles as electron mediator, photosensitizer, spectral converter, or photocatalyst. Characterized by low cost, easy preparation, water soluble and nontoxic, CQDs have served as a common replacement for toxic heavy metal-based QDs and high-expense noble metals as co-catalysts. In addition, benefiting from the generally simple and economic synthesis of CQDs out of a wide spectrum of biomass carbon sources, the application of CQDs as photocatalytic component is of great potential in view of large-scale production especially for technological purpose.

Acknowledgements

This work was supported by the National Natural Science Foundation of China (51372266, 51572286, and 21503266) and the Outstanding Youth Fund of Jiangsu Province (BK20160011).

Author details

Shan Cong* and Zhigang Zhao

*Address all correspondence to: Scong2012@sinano.ac.cn

Key Lab of Nanodevices and Applications, Suzhou Institute of Nano-Tech and Nano-Bionics, Chinese Academy of Sciences (CAS), SuzhouPR, China

References

[1] Xu X, Ray R, Gu Y, Ploehn HJ, Gearheart L, Raker K, Scrivens WA. Electrophoretic analysis and purification of fluorescent single-walled carbon nanotube fragments. Journal of the American Chemical Society. 2004;**126**(40):12736-12737. DOI: 10.1021/ja040082h

[2] Zhou J, Booker C, Li R, Zhou X, Sham TK, Sun X, Ding Z. An electrochemical avenue to blue luminescent nanocrystals from multiwalled carbon nanotubes (MWCNTs). Journal of the American Chemical Society. 2007;**129**(4):744-745. DOI: 10.1021/ja0669070

[3] Zhang J, Yu SH. Carbon dots: Large-scale synthesis, sensing and bioimaging. Materials Today. 2016;**19**(7):382-393. DOI: 10.1016/j.mattod.2015.11.008

[4] Yuan F, Li S, Fan Z, Meng X, Fan L, Yang S. Shining carbon dots: Synthesis and biomedical and optoelectronic. Nano Today. 2016;**11**(5):565-586. DOI: 10.1016/j.nantod.2016.08.006

[5] Li H, Kang Z, Liu Y, Lee ST. Carbon nanodots: Synthesis, properties and applications. Journal of Materials Chemistry. 2012;**22**:24230-24253. DOI: 10.1039/C2JM34690G

[6] Lim SY, Shen W, Gao Z. Carbon quantum dots and their applications. Chemical Society Reviews. 2015;**44**:362-381. DOI: 10.1039/C4CS00269E

[7] Wang Y, Hu A. Carbon quantum dots: Synthesis, properties and applications. Journal of Materials Chemistry C. 2014;**2**:6921-6939. DOI: 10.1039/c4tc00988f

[8] Wang R, Lu KQ, Tang ZR, Xu YJ. Recent progress in carbon quantum dots: Synthesis, properties and applications in photocatalysis. Journal of Materials Chemistry A. 2015; **5**:3717-3734. DOI: 10.1039/c6ta08660h

[9] Zheng XT, Ananthanarayanan A, Luo KQ, Chen P. Glowing graphene quantum dots and carbon dots: Properties, syntheses, and biological applications. Small. 2015;**11**(14):1620-1636. DOI: 10.1002/smll.201402648

[10] Lu J, Yang J-X, Wang J, Lim A, Wang S, Loh KP. One-pot synthesis of fluorescent carbon nanoribbons, nanoparticles, and graphene by the exfoliation of graphite in ionic liquids. ACS Nano. 2009;**3**(8):2367-2375. DOI: 10.1021/nn900546b

[11] Pan D, Zhang J, Li Z, Wu M. Hydrothermal route for Cutting graphene sheets into blue-luminescent graphene quantum dots. Advanced Materials. 2009;**22**(6):734-738. DOI: 10.1002/adma.200902825

[12] Tao H, Yang K, Ma Z, Wan J, Zhang Y, Kang Z, Liu Z. In vivo NIR fluorescence imaging, biodistribution, and toxicology of photoluminescent carbon dots produced from carbon nanotubes and graphite. Small. 2012;**8**(2):281-290. DOI: 10.1002/smll.201101706

[13] Li Y, Hu Y, Zhao Y, Shi G, Deng L, Hou Y, Qu L. An electrochemical avenue to green-luminescent graphene quantum dots as potential electron-Acceptors for photovoltaics. Advanced Materials. 2011;**23**(6):776-780. DOI: 10.1002/adma.201003819

[14] Shinde DB, Pillai VK. Electrochemical preparation of luminescent graphene quantum dots from multiwalled carbon nanotubes. Chemistry—A European Journal. 2012;**18** (39):12522-12528. DOI: 10.1002/chem.201201043

[15] Lu Q, Wu C, Liu D, Wang H, Su W, Li H, Zhang Y, Yao S. A facile and simple method for synthesis of graphene oxide quantum dots from black carbon. Green Chemistry. 2017; **19**:900-904. DOI: 10.1039/C6GC03092K

[16] Qiao Z-A, Wang Y, Gao Y, Li H, Dai T, Liu Y, Huo Q. Commercially activated carbon as the source for producing multicolor photoluminescent carbon dots by chemical oxidation. Chemical Communications. 2010;**46**:8812-8814. DOI: 10.1039/C0CC02724C

[17] Yu H, Li X, Zeng X, Lu Y. Preparation of carbon dots by non-focusing pulsed laser irradiation in toluene. Chemical Communications. 2016;**52**:819-822. DOI: 10.1039/C5CC08384B

[18] Li JY, Liu Y, Shu QW, Liang JM, Zhang F, Chen XP, Deng XY, Swihart MT, Tan KJ. One-pot hydrothermal synthesis of carbon dots with efficient up- and down-converted photoluminescence for the sensitive detection of morin in a dual-readout assay. Langmuir. 2017;**33**(4):1043-1050. DOI: 10.1021/acs.langmuir.6b04225

[19] Deng J, Lu Q, Mi N, Li H, Liu M, Xu M, Tan L, Xie Q, Zhang Y, Yao S. Electrochemical synthesis of carbon Nanodots directly from alcohols. Chemistry—A European Journal. 2014;**20**(17):4993-4999. DOI: 10.1002/chem.201304869

[20] Sun S, Zhang L, Jiang K, Aiguo W, Lin H. Toward high-efficient red emissive carbon dots: Facile preparation, unique properties, and applications as multifunctional theranostic agents. Chemistry of Materials. 2016;**28**(23):8659-8668. DOI: 10.1021/acs.chemmater.6b03695

[21] Chen X, Zhang W, Wang Q, Fan J. C_8-structured carbon quantum dots: Synthesis, blue and green double luminescence, and origins of surface defects. Carbon. 2014;**79**:165-173. DOI: 10.1016/j.carbon.2014.07.056

[22] Yang Z-C, Wang M, Yong AM, Wong SY, Zhang X-H, Tan H, Chang AY, Li X, Wang J. Intrinsically fluorescent carbon dots with tunable emission derived from hydrothermal treatment of glucose in the presence of monopotassium phosphate. Chemical Communications. 2011;**47**:11615-11617. DOI: 10.1039/C1CC14860E

[23] da Silva Souza DR, de Mesquita JP, Lago RM, Caminhas LD, Pereira FV. Cellulose nanocrystals: A versatile precursor for the preparation of different carbon structures and luminescent carbon dots. Industrial Crops and Products. 2016;**93**:121-128. DOI: 10.1016/j.indcrop.2016.04.073

[24] Choi Y, Thongsai N, Chae A, Jo S, Kang EB, Paoprasert P, Park SY, In I. Microwave-assisted synthesis of luminescent and biocompatible lysine-based carbon quantum dots. Journal of Industrial and Engineering Chemistry. 2017;**47**:329-335. DOI: 10.1016/j.jiec.2016.12.002

[25] Sahu S, Behera B, Maiti TK, Mohapatra S. Simple one-step synthesis of highly luminescent carbon dots from orange juice: Application as excellent bio-imaging agents. Chemical Communications. 2012;**48**:8835-8837. DOI: 10.1039/C2CC33796G

[26] Wang J, Wang C-F, Chen S. Amphiphilic egg-derived carbon dots: Rapid plasma fabrication, pyrolysis process, and multicolor printing patterns. Angewandte Chemie. 2012;**124**(37):9431-9435. DOI: 10.1002/ange.201204381

[27] Guo Y, Zhang L, Cao F, Leng Y. Thermal treatment of hair for the synthesis of sustainable carbon quantum dots and the applications for sensing Hg^{2+}. Scientific Reports. 2016;**6**:35795. DOI: 10.1038/srep35795

[28] Bao L, Zhang Z-L, Tian Z-Q, Li Z, Liu C, Yi L, Qi B, Pang D-W. Electrochemical tuning of luminescent carbon nanodots: From preparation to luminescence mechanism. Advanced Materials. 2011;**23**(48):5801-5806. DOI: 10.1002/adma.201102866

[29] Tan X, Li Y, Li X, Zhou S, Fan L, Yang S. Electrochemical synthesis of small-sized red fluorescent graphene quantum dots as a bioimaging platform. Chemical Communications. 2015;**51**:2544-2546. DOI: 10.1039/C4CC09332A

[30] Li H, He X, Kang Z, Huang H, Liu Y, Liu J, Lian S, Tsang CHA, Yang X, Lee S-T. Water-soluble fluorescent carbon quantum dots and photocatalyst design. Angewandte Chemie, International Edition. 2010;**49**(26):4430-4434. DOI: 10.1002/anie.200906154

[31] Li Y, Shu H, Niu X, Wang J. Electronic and optical properties of edge-functionalized graphene quantum dots and the underlying mechanism. Journal of Physical Chemistry C. 2015;**119**(44):24950-24957. DOI: 10.1021/acs.jpcc.5b05935

[32] Li X, Lau SP, Tang L, Ji R, Yang P. Sulphur doping: A facile approach to tune the electronic structure and optical properties of graphene quantum dots. Nanoscale. 2014;**6**:5323-5328. DOI: 10.1039/C4NR00693C

[33] Lin L, Zhang S. Creating high yield water soluble luminescent graphene quantum dots via exfoliating and disintegrating carbon nanotubes and graphite flakes. Chemical Communications. 2012;**48**:10177-10179. DOI: 10.1039/C2CC35559K

[34] Peng H, Travas-Sejdic J. Simple aqueous solution route to luminescent carbogenic dots from carbohydrates. Chemistry of Materials. 2009;**21**(23):5563-5565. DOI: 10.1021/cm901593y

[35] Dan Q, Zheng M, Peng D, Zhou Y, Zhang L, Di L, Tan H, Zhao Z, Xie Z, Sun Z. Highly luminescent S, N co-doped graphene quantum dots with broad visible absorption bands for visible light photocatalysts. Nanoscale. 2013;**5**:12272-12277. DOI: 10.1039/C3NR04402E

[36] Liu R, Dongqing W, Liu S, Koynov K, Knoll W, Li Q. An aqueous route to multicolor photoluminescent carbon dots using silica spheres as carriers. Angewandte Chemie. 2009;**121**(25):4668-4671. DOI: 10.1002/ange.200900652

[37] Li C, Meziani MJ, Sahu S, Sun Y-P. Photoluminescence properties of graphene versus other carbon nanomaterials. Accounts of Chemical Research. 2013;**46**(1):171-180. DOI: 10.1021/ar300128j

[38] Li C, Wang X, Meziani MJ, Fushen L, Wang H, Luo PG, Yi L, Harruff BA, Monica Veca L, Murray D, Xie S-Y, Sun Y-P. Carbon dots for multiphoton bioimaging. Journal of the American Chemical Society. 2007;**129**(37):11318-11319. DOI: 10.1021/ja073527l

[39] Gan Z, Xinglong W, Zhou G, Shen J, Chu PK. Is there real upconversion photoluminescence from graphene quantum dots? Advanced Optical Materials. 2013;**1**(8):554-558. DOI: 10.1002/adom.201300152

[40] Shen J, Zhu Y, Chen C, Yang X, Li C. Facile preparation and upconversion luminescence of graphene quantum dots. Chemical Communications. 2011;**47**:2580-2582. DOI: 10.1039/C0CC04812G

[41] Wen X, Pyng Y, Toh Y-R, Ma X, Tang J. On the upconversion fluorescence in carbon nanodots and graphene quantum dots. Chemical Communications. 2014;**50**:4703-4706. DOI: 10.1039/c4cc01213e

[42] Miao X, Ji Z, Wu J, Shen X, Wang J, Kong L, Liu M, Song C. g-C3N4/AgBr nanocomposite decorated with carbon dots as a highly efficient visible-light-driven photocatalyst. Journal of Colloid and Interface Science. 2017;**502**:24-32. DOI: 10.1016/j.jcis.2017.04.087

[43] Huang Y, Liang Y, Rao Y, Zhu D, Cao J-j, Shen Z, Ho W, Lee SC. Environment-friendly carbon quantum dots/$ZnFe_2O_4$ photocatalysts: Characterization, biocompatibility, and mechanisms for NO removal. Environmental Science & Technology. 2017;**51**(5):2924-2933. DOI: 10.1021/acs.est.6b04460

[44] Xiuqin W, Zhao J, Guo S, Wang L, Shi W, Huang H, Liu Y, Kang Z. Carbon dot and $BiVO_4$ quantum dot composites for overall water splitting via a two-electron pathway. Nanoscale. 2016;**8**:17314-17321. DOI: 10.1039/C6NR05864G

[45] Zhang J, Abbasi F, Claverie J. An efficient templating approach for the synthesis of redispersible size-controllable carbon quantum dots from graphitic polymeric micelles. Chemistry—A European Journal. 2015;**21**(43):15142-15147. DOI: 10.1002/chem.201502158

[46] Qiong W, Li W, Yanjiao W, Huang Z, Liu S. Pentosan-derived water-soluble carbon nano dots with substantial fluorescence: Properties and application as a photosensitizer. Applied Surface Science. 2014;**315**:66-72. DOI: 10.1016/j.apsusc.2014.06.127

[47] Huijun Y, Zhao Y, Zhou C, Shang L, Peng Y, Cao Y, Li-Zhu W, Tunga C-H, Zhang T. Carbon quantum dots/TiO_2 composites for efficient photocatalytic hydrogen evolution. Journal of Materials Chemistry A. 2014;**2**:3344-3351. DOI: 10.1039/C3TA14108J

[48] Liu Q, Chen T, Guo Y, Zhang Z, Fang X. Ultrathin g-C_3N_4 nanosheets coupled with carbon nanodots as 2D/0D composites for efficient photocatalytic H_2 evolution. Applied Catalysis B: Environmental. 2016;**193**:248-258. DOI: 10.1016/j.apcatb.2016.04.034

[49] Ke J, Li X, Zhao Q, Liu B, Liu S, Wang S. Upconversion carbon quantum dots as visible light responsive component for efficient enhancement of photocatalytic performance. Journal of Colloid and Interface Science. 2017;**496**:425-433. DOI: 10.1016/j.jcis.2017.01.121

[50] Zhang H, Zhao L, Geng F, Guo L-H, Wan B, Yang Y. Carbon dots decorated graphitic carbon nitride as an efficient metal-free photocatalyst for phenol degradation. Applied Catalysis B: Environmental. 2016;**180**:656-662. DOI: 10.1016/j.apcatb.2015.06.056

[51] Di J, Xia J, Chen X, Ji M, Yin S, Qi Z, Li H. Tunable oxygen activation induced by oxygen defects in nitrogen doped carbon quantum dots for sustainable boosting photocatalysis. Carbon. 2017;**114**:601-607. DOI: 10.1016/j.carbon.2016.12.030

[52] Yu S, Lee SY, Umh HN, Yi J. Energy conversion of sub-band-gap light using naked carbon nanodots and rhodamine B. Nano Energy. 2016;**26**:479-487. DOI: 10.1016/j.nanoen.2016.06.008

[53] Wu W, Zhan L, Fan W, Song J, Li X, Li Z, Wang R, Zhang J, Zheng J, Wu M, Zeng H. Cu–N dopants boost electron transfer and photooxidation reactions of carbon dots. Angewandte Chemie, International Edition. 2015;**54**(22):6540-6544. DOI: 10.1002/anie.201501912

[54] Martindale BCM, Hutton GAM, Caputo CA, Prantl S, Godin R, Durrant JR, Reisner E. Enhancing light absorption and charge transfer efficiency in carbon dots through graphitization and core nitrogen doping. Angewandte Chemie, International Edition. 2017;**56**(23):6459-6463. DOI: 10.1002/anie.201700949

[55] Yeh TF, Teng CY, Chen SJ, Teng H. Nitrogen-doped graphene oxide quantum dots as photocatalysts for overall water-splitting under visible light illumination. Advanced Materials. 2014;**26**(20):3297-3303. DOI: 10.1002/adma.201305299